

Coherent Population Trapping of Electron Spins in a High-Purity n -Type GaAs Semiconductor

Kai-Mei C. Fu,^{1,*} Charles Santori,² Colin Stanley,³ M. C. Holland,³ and Yoshihisa Yamamoto^{1,†}

¹Quantum Entanglement Project, ICORP, JST, Edward L. Ginzton Laboratory, Stanford University, Stanford, California 94305-4085, USA

²Quantum Science Research, Hewlett-Packard Laboratories, 1501 Page Mill Road, MS1123, Palo Alto, California 94304, USA

³Department of Electronics and Electrical Engineering, Oakfield Avenue, University of Glasgow, Glasgow, G12 8LT, United Kingdom
(Received 31 March 2005; published 27 October 2005)

In high-purity n -type GaAs under a strong magnetic field, we are able to isolate a lambda system composed of two Zeeman states of neutral-donor-bound electrons and the lowest Zeeman state of bound excitons. When the two-photon detuning of this system is zero, we observe a pronounced dip in the excited-state photoluminescence, indicating the creation of the coherent population-trapped state. Our data are consistent with a steady-state three-level density-matrix model. The observation of coherent population trapping in GaAs indicates that this and similar semiconductor systems could be used for various electromagnetically induced transparency type experiments.

DOI: 10.1103/PhysRevLett.95.187405

PACS numbers: 78.55.Cr, 42.50.Gy, 71.35.-y, 78.67.-n

In the past decade, great steps have been made toward the coherent control of light using techniques based on electromagnetically induced transparency (EIT) [1]. Light has been slowed by 7 orders of magnitude [2], stored and released on command [3–5], and coherently manipulated while stored in atomic states [6,7]. The applications of an integrated EIT system for quantum information processing are numerous: robust entanglement creation for quantum repeaters [8], single photon detection [9] and single photon storage [4,10] for linear optics quantum computation [11], and the creation of large optical nonlinearities [12] for photonic gates in nonlinear optics quantum computation [13,14].

EIT is based on the effect of coherent population trapping, which was first observed in the 1970s in atomic gases [15,16]. In a three-level Λ system, a probe field with Rabi frequency Ω_p couples states $|1\rangle$ and $|3\rangle$, and a coupling field with Rabi frequency Ω_c couples states $|2\rangle$ and $|3\rangle$ [Fig. 1(a)]. Optical pumping leads to a coherent superposition of states $|1\rangle$ and $|2\rangle$ that is decoupled from $|3\rangle$ due to a quantum interference between the two transitions. The crucial condition for coherent population trapping is that the decoherence rate γ_{12} between states $|1\rangle$ and $|2\rangle$ is slow compared to the radiative decay rate of $|3\rangle$. Furthermore, for photon-storage applications, γ_{12}^{-1} determines how long quantum information can be stored [3].

Long decoherence times, which naturally arise in atomic systems [4], are also possible in solids [17–19]. EIT has been observed in rare-earth doped insulators [5], nitrogen-vacancy centers in diamond [17], and in the transient optical response of GaAs quantum wells [20]. Here we consider electron spins bound to neutral donors (D^0) in a semiconductor, a system that could offer some unique advantages. For example, the optical transitions to the donor-bound-exciton states feature a small inhomogeneous broadening (2 GHz) combined with a large oscillator strength (1 ns radiative lifetime [21]). Furthermore, the

ground state is long lived, unlike the exciton states used in previous semiconductor EIT experiments [20]. Finally, donor impurities can easily be integrated into monolithic microcavities. In this Letter, we report the observation of coherent population trapping in an ensemble of D^0 spins, demonstrating that a Λ system can be optically addressed and manipulated. While the degree of ground-state coherence currently obtainable is small, it is thought to be limited mainly by inhomogeneous broadening of the electron-Zeeman splitting, which can hopefully be remedied in pulsed experiments with spin-echo techniques.

The energy level structure of a neutral donor is shown in Fig. 1(b). Because of the small electron effective mass and high dielectric constant of GaAs, the wave function of a neutral-donor-bound electron (D^0) extends over many lattice sites and is well described by the hydrogenic wave

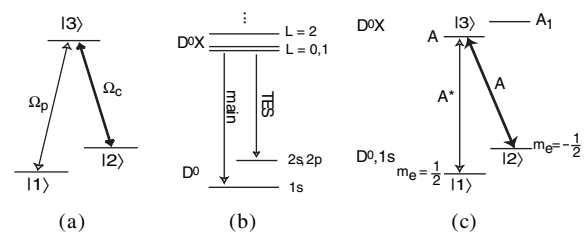


FIG. 1. (a) 3-level Λ system. (b) Energy level diagram of the D^0X and D^0 states at 0 T. In all experiments, we resonantly excite the main transitions and probe the excited-state population via the TES photoluminescence. (c) Energy level diagram of D^0 $1s$ and lowest two D^0X states in an applied magnetic field. A complete energy diagram of the GaAs D^0X states in a magnetic field is found in Ref. [23]. In the spherical approximation, state A corresponds to hole state $L = 0$, $m_h = -\frac{3}{2}$ and state A_1 corresponds to $L = 1$, $m_h = -\frac{1}{2}$. Transition A^* is allowed due to the lack of spherical symmetry in the crystal lattice. To create a population-trapped state, we apply a strong coupling field to transition A and a weak probe field to A^* .

function with a 100 \AA Bohr radius [22]. With an applied magnetic field, the $1s$ state splits into the two electron-Zeeman spin states which are labeled $|1\rangle$ and $|2\rangle$ in Fig. 1(c). The excited states consist of an electron-hole pair, or exciton, bound to the D^0 center. This donor-bound-exciton complex (D^0X), consisting of two electrons in a spin-singlet state, a hole with quasi-spin-3/2, and the donor impurity, can be resonantly excited from the D^0 state. At zero magnetic field, the D^0X is composed of closely spaced orbital angular momentum states [Fig. 1(b)]. In a magnetic field, each of the D^0X states splits into the four hole-Zeeman spin states. In Fig. 1(c) we identify the lowest-energy D^0X states as A and A_1 following Ref. [23]. We denote transitions to the D^0 state $|m_e = -\frac{1}{2}\rangle$ with a label only (e.g., A) and transitions to the state $|m_e = \frac{1}{2}\rangle$ with an asterisk (e.g., A^*). Although the D^0X predominately relaxes to the $D^0 1s$ state, there is a small probability it will decay to an excited orbital D^0 state. These transitions are called “two electron satellites” or TES [Fig. 1(b)].

Our sample consisted of a $10 \text{ }\mu\text{m}$ GaAs layer on a $4 \text{ }\mu\text{m}$ $\text{Al}_{0.3}\text{Ga}_{0.7}\text{As}$ layer grown by molecular-beam epitaxy on a GaAs substrate. The sample had a donor concentration of $\sim 5 \times 10^{13} \text{ cm}^{-3}$. We mounted the sample strain-free in a magnetic cryostat in the Voigt ($\vec{k} \perp \vec{B}$) geometry. A photoluminescence (PL) spectrum of the D^0X emission at 7 T and 1.5 K is shown in Fig. 2. With above-band excitation, the A and A^* transitions are clearly resolved. In addition, we can identify the TES lines associated with state A by resonantly exciting the A or A^* transitions and observing enhancements in the associated TES lines.

Coherent population trapping can be observed as a decrease in the excited-state population when two-photon resonance occurs. In our experiment, we monitor the excited-state population using the TES fluorescence. In photoluminescence excitation (PLE) scans, an external-cavity diode laser resonant with the A transition (817.448 nm) [see Fig. 1(c)] provides the “coupling” field, and a ring Ti:sapphire laser, scanned across the A^* tran-

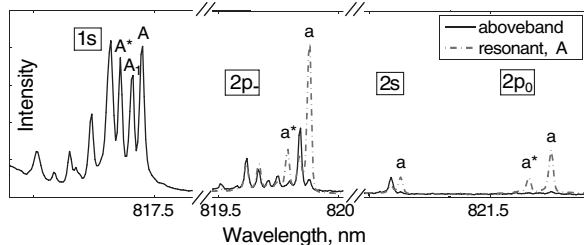


FIG. 2. Above-band and resonant excitation photoluminescence spectra of D^0X . Transitions A and A^* are clearly resolved. With resonant excitation of transition A , the TES lines associated with state A (labeled a , a^*) are noticeably enhanced. A detailed assignment of the D^0X excited states can be found in Ref. [23]. Above-band TES intensities are 10 times the actual intensity. Resolution is spectrometer limited.

sition (817.358 nm), provides the “probe” field. The scan resolution was measured using an optical spectrum analyzer to be better than 10 MHz. The energy splitting between the two transitions corresponds to the 7 T electron-Zeeman energy. The observed g factor $|g| = 0.41$ is close to the previously measured $g = -0.43$ determined by the $2p_-$ splitting [23].

The results from a representative scan are shown in Fig. 3. We discuss three scenarios: probe-laser only excitation, two-laser excitation detuned from resonance, and two-laser excitation on two-photon resonance. With the probe laser only, the PLE spectrum gives a linewidth of only 2 GHz. The data fit a Lorentzian line shape extremely well and indicate that there is little inhomogeneous broadening. The emission intensity is weak due to optical pumping of most of the electron population into state $|2\rangle$, which for the probe laser only is a dark state. With both lasers exciting the sample but detuned from two-photon resonance, the emission becomes much stronger since in this case there is no dark state. When the probe and coupling lasers are brought into two-photon resonance, a pronounced and narrow reduction of the emission intensity is observed as a new dark state is formed which is a coherent superposition of states $|1\rangle$ and $|2\rangle$.

The decrease in the excited-state population observed on two-photon resonance is incomplete because of decoher-

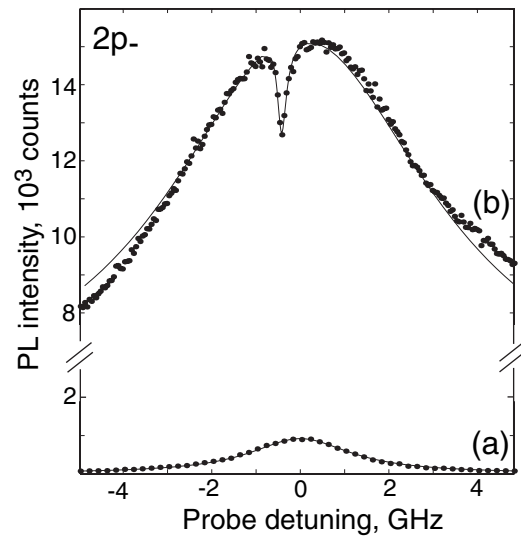


FIG. 3. (a) Probe only PLE scan over A^* transition. PL is collected from the $2p_-$ “a” TES line. Probe-laser intensity is $\sim 0.15 \text{ W/cm}^2$. (b) PLE scan over the A^* transition with the coupling-laser resonant on the A transition. Coupling intensity is $\sim 2.5 \text{ W/cm}^2$. A dip in the PLE intensity at zero two-photon detuning due to coherent population trapping is observed. Identical behavior is also observed for the $2p_0$ and $2s$ TES lines. The solid line is a theoretical fit by the three-level density-matrix model described in the text. The fitting parameters are $\Omega_c = 650 \text{ MHz}$, $\Omega_p = 16 \text{ MHz}$, $\Gamma_{21} = (2.6 \text{ }\mu\text{s})^{-1}$, $\gamma_{3a} = 4.6 \text{ GHz}$, $\gamma_{3b} = 22 \text{ GHz}$, $\Gamma_{32} = 1 \text{ ns}^{-1}$, $\Gamma_{31} = 0.08\Gamma_{32}$, $\gamma_{12} = (1.7 \text{ ns})^{-1}$.

ence and population relaxation between levels $|1\rangle$ and $|2\rangle$. The results can be understood in terms of a 3-level system interacting with a reservoir, described by the density-matrix master equation:

$$\frac{\partial}{\partial t}\rho = \frac{1}{i\hbar}[H, \rho] - \mathcal{L}(\rho) = 0,$$

in which H is the Hamiltonian of the system and $\mathcal{L}(\rho)$ is the Lindbladian operator describing the decoherence processes. In the interaction picture and rotating wave ap-

proximation,

$$H = -\hbar \begin{pmatrix} 0 & 0 & \frac{\Omega_p^*}{2} \\ 0 & \delta & \frac{\Omega_c^*}{2} \\ \frac{\Omega_p}{2} & \frac{\Omega_c}{2} & \Delta \end{pmatrix},$$

in which Δ is the probe detuning and δ is the two-photon detuning from the electron-Zeeman splitting. The relaxation operator $\mathcal{L}(\rho)$ is given by

$$\mathcal{L}(\rho) = \begin{pmatrix} -\Gamma_{12}\rho_{11} + \Gamma_{21}\rho_{22} + \Gamma_{31}\rho_{33} & -(\frac{\Gamma_{12}+\Gamma_{21}}{2} + \gamma_2)\rho_{12} & -(\frac{\Gamma_{12}+\Gamma_{31}+\Gamma_{32}}{2} + \gamma_{3a,3b})\rho_{13} \\ -(\frac{\Gamma_{12}+\Gamma_{21}}{2} + \gamma_2)\rho_{21} & \Gamma_{12}\rho_{11} - \Gamma_{21}\rho_{22} + \Gamma_{32}\rho_{33} & -(\frac{\Gamma_{21}+\Gamma_{31}+\Gamma_{32}}{2} + \gamma_{3a,3b})\rho_{23} \\ -(\frac{\Gamma_{12}+\Gamma_{31}+\Gamma_{32}}{2} + \gamma_{3a,3b})\rho_{31} & -(\frac{\Gamma_{21}+\Gamma_{31}+\Gamma_{32}}{2} + \gamma_{3a,3b})\rho_{32} & -(\Gamma_{31} + \Gamma_{32})\rho_{33} \end{pmatrix}, \quad (1)$$

in which Γ_{12} ($\Gamma_{21} = \Gamma_{12}e^{E_{12}/kT}$) is the longitudinal relaxation rate from $|1\rangle \rightarrow |2\rangle$ ($|2\rangle \rightarrow |1\rangle$), Γ_{31} (Γ_{32}) is the radiative relaxation from $|3\rangle \rightarrow |1\rangle$ ($|3\rangle \rightarrow |2\rangle$), γ_2 is the transverse relaxation rate between $|1\rangle$ and $|2\rangle$, and γ_{3a} (γ_{3b}) is the level $|3\rangle$ dephasing without (with) the coupling field. With these definitions, the total lower-level decoherence rate is given by $\gamma_{12} = \frac{1}{2}(\Gamma_{12} + \Gamma_{21}) + \gamma_2$.

Fitting ρ_{33} from the above model to the measured PLE curve gives reasonable agreement, as shown in Fig. 3. The only parameter that must be changed to fit simultaneously both (a) the single laser and (b) two-laser scans is the level $|3\rangle$ dephasing rate. The fit indicates slow (μ s) electron population-relaxation rates and fast (1–2 ns) electron decoherence rates in our system. Thus, the system exhibits a lower-level dephasing rate on the same order as the excited-state radiative lifetime (1 ns). From this fit, we can also obtain the ratio of the two-state coherence, ρ_{12} , to the ideal case $\rho_{12,\text{ideal}} = \Omega_p\Omega_c/(\Omega_p^2 + \Omega_c^2)$ and find that $\rho_{12}/\rho_{12,\text{ideal}} = 0.23$. In the weak probe limit ($\Omega_p \ll \Omega_c, \Gamma_{31}, \Gamma_{32}$), ρ_{12} reduces to

$$\rho_{12} \approx \frac{\Omega_p\Omega_c}{4\gamma_{13}\gamma_{12} + \Omega_c^2},$$

in which γ_{13} (γ_{12}) is the total decay rate for ρ_{13} (ρ_{12}) given in Eq. (1). From this relationship, it is evident that the coherence of this system is currently limited by the short lower-level decoherence time as well as additional dephasing of state $|3\rangle$.

Additional measurements to verify the theoretically expected behavior are shown in Fig. 4. In Fig. 4(a), PLE scans were performed at several coupling intensities. As the coupling intensity increases, the population-trapped window at zero two-photon detuning becomes relatively wider and deeper as expected. The data fit our theoretical model if the lower-level population-relaxation rate is allowed to increase with increased coupling field intensity. This increase could be due to sample heating at large coupling-laser powers. In our sample, the GaAs substrate was not

removed and absorbs all of the incident radiation. If we assume a one-phonon spin-orbit relaxation process [24,25], we are able to simultaneously fit the coupling power dependence series by varying only the sample temperature from 1.5 to 6 K. In a second experiment [Fig. 4(b)], the two lasers are tuned to different excited states and the PLE dip is not observed. In this case, the probe laser is tuned to the A_1^* transition and the coupling laser is tuned to the A transition [see Fig. 1(c)]. As in the previous case, if only the probe laser is applied, population becomes depleted from state $|1\rangle$ and the PLE intensity is weak. The coupling laser repopulates this state, and the PLE intensity is enhanced. The absence of the dip in this experiment as well as the narrow dip in the Λ system ($\text{FWHM} \ll \text{homoge-}$

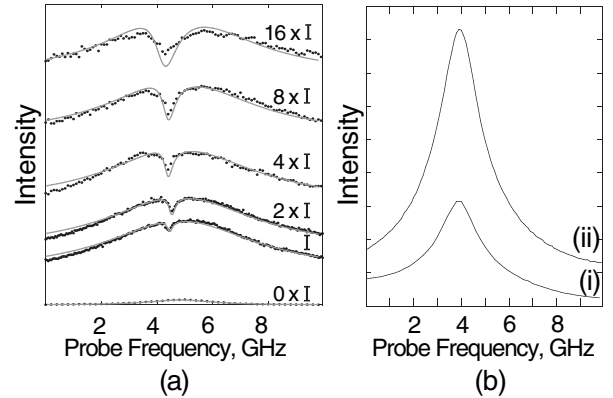


FIG. 4. (a) PLE scans with varying coupling field intensities. $I \sim 1 \text{ W/cm}^2$. The dip becomes wider and deeper relative to the wings of the curve as the coupling field is increased. The only fitting parameter varied between the 5 two-laser scans is T ($\Gamma_{12} \propto (e^{\Delta E/kT} - 1)^{-1}$). In order of increasing coupling intensity, $T = 1.5, 1.5, 2.0, 3.1, 4.6, 6.0 \text{ K}$. (b) Incoherent optical pumping experiment with (i) coupling laser off, (ii) coupling laser on. The coupling laser is tuned to transition A . The probe laser is scanned over A_1^* [see Fig. 1(c)]. An enhancement of the PLE intensity in the two-laser case is observed without a dip at zero detuning.

neous broadening) indicate that our results cannot be explained by standard spectral hole burning.

We observe only a modest suppression of the excited-state population. This is due to the 1–2 ns inhomogeneous decoherence time T_2^* . At the extremely low densities ($\sim 5 \times 10^{13} \text{ cm}^{-3}$) in our sample, the nuclear-electron hyperfine interaction becomes very efficient [26]. At these densities, the donor electrons are well localized and do not interact with each other. At 2 K the nuclei are essentially unpolarized, and theoretical calculations predict nanosecond T_2^* due to the random nuclear states [27]. Experimentally, a 5 ns T_2^* has been measured in *n*-type GaAs with $n \sim 3 \times 10^{14} \text{ cm}^{-3}$ via optically detected electron-spin resonance [28]. This result is consistent with our value given our sample's lower donor density. Additionally, we find that, if we increase the temperature of our sample up to 6 K, although the overall PLE intensity decreases dramatically, the width of the dip does not change significantly. This indicates that T_2^* in our system is not temperature dependent and is consistent with the nuclear-electron hyperfine decoherence model.

Although the *inhomogeneous* T_2^* limits the depth of the population-trapped dip, in an EIT-type experiment with pulsed lasers and electron-spin-echo techniques, the storage time should be limited by the *homogeneous* decoherence time T_2 . T_2 of electron spins in GaAs has not been measured but could be close to the population-relaxation time, on the order of microseconds. It has also been proposed that further improvements of storage time could be made by transferring the electron-spin coherence to the nuclear spins. If this is achieved, a storage time on the order of seconds may be feasible [29].

In summary, we have observed coherent population trapping of donor-bound electrons in GaAs. To our knowledge, this is the first demonstration of a Λ system in a semiconductor that utilizes the true electron ground states. In addition, due to the substitutional nature of donor impurities and high crystal quality, this system has little inhomogeneous broadening in the optical transitions. Although current population trapping is limited by a short T_2^* , there exist several possible ways to engineer this system for long T_2 and storage times. Spin-echo techniques and electron to nuclear information transfer should be able to extend possible storage times by orders of magnitude in GaAs. Additionally, the D^0X system exists in every semiconductor. Thus, a crystal composed of nuclear spin-0 elements would significantly extend the storage lifetime. We also note that larger band gap semiconductors have larger effective masses, larger D^0 binding energies, and, thus, larger D^0X binding energies [30], which allow higher temperature operation.

Financial support was provided by the MURI Center for photonic quantum information systems (ARO/ARDA Program No. DAAD19-03-1-0199) and NTT Basic Research Laboratories. This material was based upon

work through the National Science Foundation Graduate program. We thank T. D. Ladd, J. R. Goldman, K. Sanaka, and S. Clark for their help with the experimental aspects of this work. We also thank S. E. Harris, D. Gammon, S. Yelin, and M. D. Lukin for the valuable discussions.

*Electronic address: kaimeifu@stanford.edu

†Also at National Institute of Informatics, Tokyo, Japan.

- [1] S. E. Harris, *Phys. Today* **50**, No. 7, 36 (1997).
- [2] L. V. Hau, S. E. Harris, Z. Dutton, and C. H. Behroozi, *Nature (London)* **397**, 594 (1999).
- [3] M. Fleischhauer and M. D. Lukin, *Phys. Rev. Lett.* **84**, 5094 (2000).
- [4] C. Liu, A. Dutton, C. H. Behroozi, and L. V. Hau, *Nature (London)* **409**, 490 (2001).
- [5] A. V. Turukhin *et al.*, *Phys. Rev. Lett.* **88**, 023602 (2002).
- [6] A. Mair, J. Hager, D. F. Phillips, R. L. Walsworth, and M. D. Lukin, *Phys. Rev. A* **65**, 031802(R) (2002).
- [7] M. Bajcsy, A. S. Zibrov, and M. D. Lukin, *Nature (London)* **426**, 638 (2003).
- [8] L.-M. Duan, M. D. Lukin, J. I. Cirac, and P. Zoller, *Nature (London)* **414**, 413 (2001).
- [9] S. E. Harris and Y. Yamamoto, *Phys. Rev. Lett.* **81**, 3611 (1998).
- [10] D. F. Phillips, A. Fleischhauer, A. Mair, R. L. Walsworth, and M. D. Lukin, *Phys. Rev. Lett.* **86**, 783 (2001).
- [11] E. Knill, R. Laflamme, and G. J. Milburn, *Nature (London)* **409**, 46 (2001).
- [12] H. Schmidt and A. Imamoglu, *Opt. Lett.* **21**, 1936 (1996).
- [13] I. L. Chuang and Y. Yamamoto, *Phys. Rev. A* **52**, 3489 (1995).
- [14] W. J. Munro *et al.*, *J. Opt. B* **7**, S135 (2005).
- [15] G. Alzetta, A. Gozzini, L. Moi, and G. Orriols, *Nuovo Cimento B* **36**, 5 (1976).
- [16] H. R. Gray, R. M. Whitley, and C. R. Stroud, Jr., *Opt. Lett.* **3**, 218 (1978).
- [17] P. R. Hemmer, A. V. Turukhin, M. S. Shahriar, and J. A. Musser, *Opt. Lett.* **26**, 361 (2001).
- [18] A. M. Tyryshkin, S. A. Lyon, A. V. Astashkin, and A. M. Raitsimring, *Phys. Rev. B* **68**, 193207 (2003).
- [19] T. A. Kennedy *et al.*, *Appl. Phys. Lett.* **83**, 4190 (2003).
- [20] M. Phillips and H. Wang, *Phys. Rev. Lett.* **89**, 186401 (2002).
- [21] C. J. Hwang, *Phys. Rev. B* **8**, 646 (1973).
- [22] B. J. Skromme *et al.*, *J. Appl. Phys.* **58**, 4685 (1985).
- [23] V. A. Karasyuk *et al.*, *Phys. Rev. B* **49**, 16381 (1994).
- [24] A. V. Khaetskii and Y. V. Nazarov, *Phys. Rev. B* **64**, 125316 (2001).
- [25] L. M. Woods, T. L. Reinecke, and Y. Lyanda-Geller, *Phys. Rev. B* **66**, 161318(R) (2002).
- [26] R. I. Dzhiyev *et al.*, *Phys. Rev. B* **66**, 245204 (2002).
- [27] I. A. Merkulov, A. L. Efros, and M. Rosen, *Phys. Rev. B* **65**, 205309 (2002).
- [28] J. S. Colton *et al.*, *Solid State Commun.* **132**, 613 (2004).
- [29] J. M. Taylor, C. M. Marcus, and M. D. Lukin, *Phys. Rev. Lett.* **90**, 206803 (2003).
- [30] J. R. Haynes, *Phys. Rev. Lett.* **4**, 361 (1960).